Heme oxygenase-1 inhibits renal tubular epithelial cell pyroptosis by regulating mitochondrial function through PINK1

HAI-BO LI[1*], YAN-SHUAI MO[2*], XI-ZHE ZHANG[1*], QI ZHOU[1], XIAO-DONG LIANG[1], JIAN-NAN SONG[1], LI-NA HOU[1], JIAN-NAN WU[1], YING GUO[1], DAN-DAN FENG[1], YI SUN[1] and JIAN-BO YU[2]

[1]Department of Anesthesiology, Chifeng Municipal Hospital, Chifeng, Inner Mongolia 024000; [2]Department of Anesthesiology and Critical Care Medicine, Tianjin Nankai Hospital, Tianjin Medical University, Tianjin 300102, P.R. China

Received September 13, 2022; Accepted February 24, 2023

DOI: 10.3892/etm.2023.11912

Abstract. Endotoxin-induced acute kidney injury (AKI) is commonly observed in clinical practice. Renal tubular epithelial cell (RTEC) pyroptosis is one of the main factors leading to the development of endotoxin-induced AKI. Mitochondrial dysfunction can lead to pyroptosis. However, the biological pathways involved in the potential lipopolysaccharide (LPS)-induced pyroptosis of RTECs, notably those associated with mitochondrial dysfunction, are poorly understood. Previous studies have demonstrated that heme oxygenase (HO)-1 confers cell protection via the induction of PTEN-induced putative kinase 1 (PINK1) expression through PTEN to regulate mitochondrial fusion/fission during endotoxin-induced AKI *in vivo*. Therefore, the present study investigated the role of HO-1/PINK1 in maintaining mitochondrial function and inhibiting the pyroptosis of RTECs exposed to LPS. Primary cultures of RTECs were obtained from wild-type (WT) and PINK1-knockout (PINK1KO) rats. An *in vitro* model of endotoxin-associated RTEC injury was established following treatment of the cells with LPS. The WT RTECs were divided into the control, LPS, Znpp + LPS and Hemin + LPS groups, and the PINK1KO RTECs were divided into the control, LPS and Hemin + LPS groups. RTECs were exposed to LPS for 6 h to assess cell viability, inflammation, pyroptosis and mitochondrial function. In the LPS-treated RTECs, the mRNA and protein expression levels of HO-1 and PINK1 were upregulated. Cell viability, adenosine triphosphate (ATP) levels and the mitochondrial oxygen consumption rate were decreased, whereas the inflammatory response, pyroptosis and mitochondrial reactive oxygen species (ROS) levels were increased. The cell inflammatory response and the induction of pyroptosis were inhibited, whereas the levels of mitochondrial ROS were decreased. In addition, the cell viability and ATP levels were increased in the WT RTECs following the upregulation of HO-1 expression. These effects were reversed by the downregulation of HO-1 expression. However, no statistically significant differences were noted between the LPS and the Hemin + LPS groups in the PINK1KO RTECs. Collectively, the findings of the present study indicate that HO-1 inhibits inflammation and regulates mitochondrial function by inhibiting the pyroptosis of LPS-exposed RTECs via PINK1.

Introduction

Acute kidney injury (AKI) induced by endotoxins is a common cause of morbidity and mortality in critically ill patients (1-3). Previous studies have demonstrated that oxidative stress and persistent inflammation can result in the necrosis and apoptosis of renal tubular epithelial cells (RTECs) (4,5). Recently, the pyroptosis of RTECs was observed in endotoxin-induced AKI *in vivo* (6). Pyroptosis is a type of programmed cell death that occurs when a cell bulks up until the cell membrane bursts, causing the release of cellular contents, which activate a potent inflammatory response (7,8). It is characterized by caspase-1 and IL-1β activation, which is associated with the release of a large number of pro-inflammatory factors. Pyroptosis is a natural immune response in the body that plays a critical role in combatting infections (9). Mitochondrial injury is related to pyroptosis (10). Endotoxin-induced AKI leads to mitochondrial fission and RTEC pyroptosis (11).

The core of cellular energy metabolism is the mitochondrion, which provides energy for cellular metabolism in the form of adenosine triphosphate (ATP). Cellular stress leads to mitochondrial damage and dysfunction, resulting in damage to the electron respiration complex, mitochondrial oxygen consumption, oxidative phosphorylation, decreased ATP synthesis and the increased production of reactive oxygen species (ROS). These processes induce programmed cell death (12). In addition, it has been shown that the tendency of RTEC mitochondria to divide may induce dysfunction.

Correspondence to: Professor Jian-Bo Yu, Department of Anesthesiology and Critical Care Medicine, Tianjin Nankai Hospital, Tianjin Medical University, 102 Sanwei Road, Nankai, Tianjin 300102, P.R. China
E-mail: 30717008@nankai.edu.cn

*Contributed equally

Key words: renal tubular epithelial cells, heme oxygenase-1, PTEN-induced putative kinase 1, mitochondrial, pyroptosis

The inhibition of the latter is the key to endogenous protection towards the treatment of AKI induced by endotoxemia (13).

Heme oxygenase (HO) is a rate-limiting enzyme used in the conversion of heme into biliverdin and bilirubin. It contains two isoforms, namely HO-1 and HO-2. HO-1 inhibits inflammatory responses, reduces oxidative stress and improves cell survival rates (14). In recent years, HO-1 has been shown to exert a protective effect on endogenous levels. HO-1 can inhibit inflammatory responses and reduce oxidative stress to improve endotoxemia-induced organ damage by regulating specific organelles, such as the mitochondria and the endoplasmic reticulum (15,16). PTEN-induced putative kinase 1 (PINK1) can clear dysfunctional mitochondria by regulating mitochondrial autophagy (17). HO-1 regulates mitochondrial fusion/fission via PINK1 to improve endotoxin-induced AKI *in vivo* (11). However, whether HO-1 regulates mitochondrial dysfunction through PINK1 *in vitro* and inhibits pyroptosis in lipopolysaccharide (LPS)-stimulated RTECs remains to be determined. In the present study, it was hypothesized that HO-1 inhibits inflammation, regulates mitochondrial function and inhibits focal prolapse, thereby reducing the damage caused to RTECs by the LPS-mediated induction of PINK1 expression.

Materials and methods

Animals. A total of 40 1-month-old Sprague-Dawley neonatal rats were purchased, including 20 wild-type (WT) neonatal rats and 20 PINK1-knockout (PINK1KO) neonatal rats. The 1-month-old male Sprague-Dawley neonatal rats (weighing 50-60 g) were provided by the Laboratory Animal Center of the Nankai Clinical Institution of Tianjin Medical University, Tianjin, China. The 1-month-old PINK1KO neonatal rats (weighing 50-60 g) were purchased from Beijing Baiao Saitu Gene Biotechnology Co. Ltd. (EGE-WL-008). PINK1 gene conditional knockout in Sprague-Dawley rats was successfully established using the CRISPR/Cas9 method (Data S1, and Figs. S1 and S2).

The WT and PINK1KO neonatal rats used in the experiments were age- and weight-matched littermates. The neonatal rats were kept alone in a cage at 23-25˚C and adapted to a 12-h light-dark cycle, 60-65% humidity, with free access to food and water.

The present study was approved by the Animal Ethical and Welfare Committee of the Institute of Radiation Medicine, Chinese Academy of Medical Sciences (no. IRM-DWLL-201907) and was performed in accordance with the ARRIVE guidelines developed by the National Center for the Replacement, Refinement, and Reduction of Animals in Research. As the neonatal rats in this experiment were sacrificed and part of the experiments were conducted in the animal laboratory of the aforementioned institution, the ethics approval for the use of animals was provided by this institution.

Cells and cell culture. The *ex vivo* primary culture of RTECs in WT rats and PINK1KO rats was performed as previously described (18). The neonatal rats (weighing 50-60 g) were anesthetized by the inhalation of 3% isoflurane until the four toes of the rats were pinched with tweezers and the rats had no reaction after pinching; the rats were then sacrificed by cervical dislocation and disinfected with 75% alcohol for 3 min. Their skin was cut open at the coastal ridge angle to expose the kidneys. The kidneys were gently removed and the ureter and blood vessels were cut; the kidneys were placed in medium containing double resistance (cat. no. 12100-500; Beijing Solarbio Science & Technology Co., Ltd.; 1% of two antibiotics, including penicillin and streptomycin). Subsequently, the kidneys were cut open, the pedicles were cut off, and the capsules were separated and removed. The medulla of the kidneys was removed and the cortex was cut and placed into a Petri dish containing double-resistance PBS (Biosharp Life Sciences). The cortex was dissected under a microscope (optical, Olympus Corporation) and the solution was filtered using 100- and 80-micron filtering screens. The filtrate containing the cells was obtained from sieve filtration, added to 50-ml centrifuge tubes, and centrifuged at 250 x g at room temperature. The supernatant was discarded and the sample was digested with collagenase for 20 min at 37˚C in a water bath (every 3-5 min and percussion). The sample was centrifuged (rotational speed, 250 x g at room temperature; duration, 5 min), the supernatant was discarded and whole medium was added at a 2:1 volume ratio. The mixture was discarded evenly with a straw to terminate the digestion, and subsequently was centrifuged at a rotational speed of 250 x g at room temperature for 5 min. The number and density of the cells were observed under a microscope (optical, Olympus Corporation) and subsequently divided into culture plates. RTECs are identified by their morphology (Data S1, and Figs. S3 and S4). The cells were cultured in an incubator at 37˚C containing a 5% CO_2. The solution was changed every 2-3 days. The cells were seeded in 96-well culture plates at a density of $4x10^4$ cells/ml. The RTECs were divided into seven groups (n=3) as follows: The WT control RTECs, LPS, zinc protoporphyrin IX (Znpp) + LPS and Hemin + LPS groups. The PINK1KO RTECs were divided into the control, LPS and Hemin + LPS groups. Normal culture was performed in the control group and 1 μg/ml LPS was added to each medium in the LPS, Znpp + LPS and Hemin + LPS groups to stimulate the RTECs. The RTECs in the Znpp + LPS and Hemin + LPS groups were treated with 10 μM of the HO-1 inhibitor, ZnPP (Sigma-Aldrich; Merck KGaA), and 20 μM of the HO-1 promoter, hemin (Sigma-Aldrich; Merck KGaA), for 30 min prior to LPS (Beijing Solarbio Science & Technology Co., Ltd.) stimulation. A flow diagram of the experiment is presented in Fig. 1.

Cell viability. The RTECs were incubated overnight in 96-well plates at a density of $4x10^4$ cells/ml at 37˚C in a cell culture incubator containing 5% CO_2. The medium was replaced with DMEM (cat. no. 8122059; Gibco; Thermo Fisher Scientific, Inc.) containing 1% FBS (cat. no. 212619; Biological Industries), which was synchronously treated for 24 h. Each group was provided with the corresponding treatment. Following incubation at 37˚C in a cell culture incubator containing 5% CO_2 for 24 h, 10 μl Cell Counting Kit-8 (CCK-8; 0.5 g/l; cat. no. BS350B, Biosharp Life Sciences) solution was added to each well, which was incubated at 37˚C for 4 h. The liquid in the plate was removed by centrifugation at 320 x g

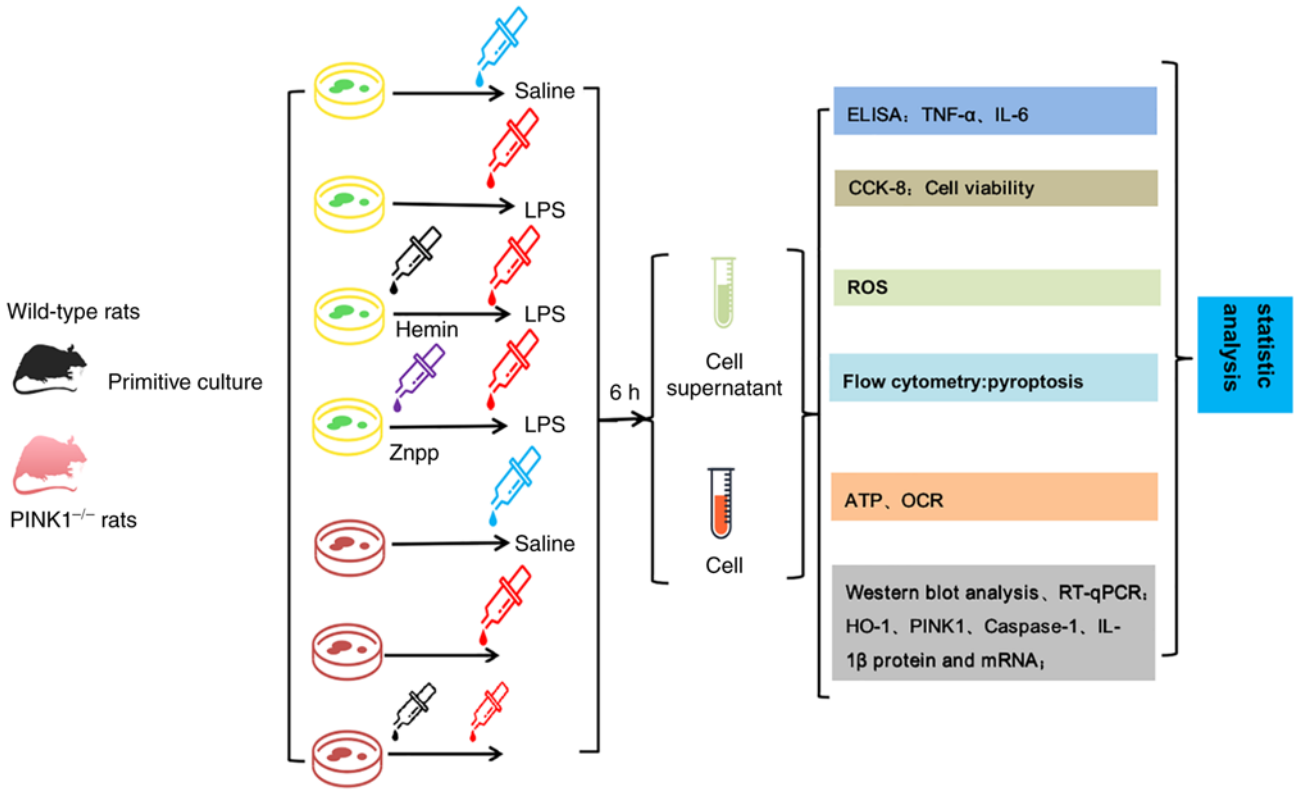

Figure 1. Flow diagram of the experiments performed in the present study.

at room temperature for 10 min. Subsequently, dimethyl sulfoxide (Beijing Solarbio Science & Technology Co., Ltd.) (100 μl/well) was added and mixed, and the optical density (OD) at 490 nm was determined using a microplate reader (Hidex), indicating cell viability.

Enzyme-linked immunosorbent assay (ELISA). ELISA kits were used to detect the levels of the inflammatory factors, IL-6 (cat. no. EK306; LiankeBio) and TNF-α (cat. no. CSB-E11987BC; Cusabio Technology, LLC) in the cell supernatant. The experimental procedures adhered to the instructions described in the manufacturer's protocol.

Determination of pyroptosis using flow cytometry. The RTECs were washed twice using cold PBS buffer, and a $1x10^6$ cells/ml cell suspension was prepared. The cell suspension (100 μl) was added to the test tube and mixed gently with fluorescence-labeled Annexin V nucleic acid dye 660 Caspase-1 Assay (cat. no. 9122; ImmunoChemistry Technologies, LLC.). The Annexin V nucleic acid dye was placed in the dark at room temperature for 15 min. The cells were initially washed with a buffer solution and the supernatant was removed when Annexin V-biotin was used for testing. Subsequently, Annexin V-fluorescein isothiocyanate (0.5 μg) was dissolved in 100 μl buffer solution, added to the tube containing the cells, and mixed gently. The buffer solution (400 μl) was added to each test tube, and the results were measured using a flow cytometer (FACSCalibur II, BD Biosciences) within 1 h. The proportion of FL4-H in each cell sample was analyzed using CellQuest 6.1 software (BD Biosciences).

Extraction of mitochondria from RTECs. The RTECs were removed, placed into the pre-cooled medium I, and washed twice. A total of 3 ml pre-cooled medium I was added to the Petri dishes. The pre-cooled homogenate (5 ml) was moved to a glass tube. In the ice bath, a 160 x g electric homogenizer was used thrice. The homogenate was pre-cooled in a 50-ml centrifuge tube, and 4 ml precooled medium I was added, followed by centrifugation at 4˚C at 40 x g for 10 min. The precipitate was discarded, and the supernatant was centrifuged at 320 x g at 4˚C for 10 min. The supernatant was subsequently removed and 5 ml medium I (including 250 μl fatty acid-free BSA) were added to the precipitate; the resulting solution was further centrifuged at 4˚C at 5,400 x g for 10 min. The supernatant was removed, precipitated and 2 ml medium II were added to the sample, including 40 μl BSA. The resulting mixture was incubated at 4˚C and centrifuged at 1,400 x g for 10 min. A total of 300 μl II suspended medium was precipitated. Of note, the entire process was performed on ice, and the reagent, centrifuge tube, and homogenizer tube were pre-cooled. The reagent preparation included the following: Medium I (0.12 M KCl, 20 mM HEPES, 5 mM $MgCl_2$, 1 mM EDTA, pH 7.4); medium II (0.3 M sucrose, 2.0 mM HEPES, 0.1 mM EDTA, pH 7.4); fatty acid-free BSA: 0.1 g/ml (cat. No. G007-1-1, Nanjing Jiancheng Bioengineering Institute).

Detection of mitochondrial ROS production. The fluorescent probe, dihydroethidium (DHE), was used for labeling ROS. The underlying principle is as follows: DHE freely enters the mitochondria through the mitochondrial membrane and is oxidized by mitochondrial ROS to form ethidium, which can bind to the chromosomal DNA and produce fluorescence.

Briefly, the cells were cultured in 96-well plates until the cultures were confluent. Subsequently, the cell suspension was incubated with 10 μM DHE at 37˚C for 30 min. A Chameleon microplate reader (Hidex) was used to monitor the DHE fluorescence at an excitation wavelength of 480 nm and an emission wavelength of 530 nm. The results were reported as the differences from the initial fluorescence. Based on the production of fluorescence and the change in its activity, the amount and change in the mitochondrial ROS content could be determined.

Determination of mitochondrial ATP. According to the instructions of the ATP detection kit (cat. No. A016-1; Nanjing Jiancheng Bioengineering Institute), an enzymolysis reaction was performed as follows: 130 μl solution A was added to a tube followed by 100 μl of sample and mixed; the reaction was performed at 37˚C for 10 min. Subsequently, 750 μl reagent were added to the tube and mixed with the sample. The tube was centrifuged at 1,000-1,800 x g at room temperature for 10 min, and the supernatant containing phosphorus was obtained. A standard phosphorus application solution (100 μl) with a concentration of 1 M/ml was added to the standard tube and 100 μl supernatant were added to the ABCDE tube. The phosphorus fixative was added to the ABCDE tube, mixed, and cooled to room temperature in a water bath at 45˚C for 20 min. At 660 nm, the optical diameter was 1 cm. The following formula was used to calculate the ATPase activity: ATPase activity (U/mg prot)=(measured OD value-control OD value)/standard OD value x concentration of standard substance (1 M/ml) x dilution ratio of samples in the reaction system x 6/concentration of protein sample to be measured (mg prot/ml).

Mitochondrial oxygen consumption. Mitochondrial oxygen consumption was monitored using the MitoXpress oxygen-sensitive probe (Cayman Chemical Company) according to the manufacturer's protocols. Briefly, 10 μl phosphorescent oxygen probe were added to each well. The wells were sealed with 100 μl ^{19}HS mineral oil (Cayman Chemical Company). The plate was measured kinetically for 30 min to ensure that the fluorescent signal was stable. Time-resolved fluorescence measurements were performed at 380 nm excitation and 650 nm emission with a delay of 30 μs and a gate time of 100 μs using a fluorescence microplate reader (Infinite M200, Tecan Group, Ltd.).

Western blot analysis. The concentration of protein from the RTECs was determined using a BCA protein quantitative kit (Thermo Fisher Scientific, Inc.), and the amount of protein loading was calculated. An appropriate amount of RIPA buffer (Beyotime Institute of Biotechnology) was used for lysis and the sample was incubated for 24 h. The protein was extracted according to the manufacturer's instructions (Thermo Fisher Scientific, Inc.). the amount of protein loaded per lane was 40 μg. Electrophoresis was performed using a 12% SDS-PAGE gel. Following PVDF membrane transfer, the membrane was incubated with 5% skimmed milk powder at 37˚C for 2 h. After washing, the membrane was incubated with the following antibodies at 4˚C overnight: HO-1 (1:500; cat. no. ab13248; Abcam), PINK1 (1:600; cat. no. ab23707; Abcam), caspase-1 (1:800; cat. no. 22915-1-AP; ProteinTech Group, Inc.), IL-1β (1:1,000; cat. no. ab9722; Abcam), and β-actin (1:1,000; cat. no. TA-09; Abcam). The following morning, the membrane was washed with TBS-Tween-20 (TBST) to remove the excess primary antibodies and incubated with a secondary rabbit or goat IgG antibody (1:3,000; cat. no. zb-2301, ZSGB Institute of Biotechnology), for 1 h at room temperature. Following additional washing with TBST, the membrane was incubated with ECL reagents (Beyotime Institute of Biotechnology) for 2-3 min at room temperature, and the signal corresponding to protein expression was developed in a darkroom on a film. The experiment was repeated thrice and the ratio of the gray values of the target protein bands to those of β-actin bands was analyzed. The area and integrated optical density of the bands were analyzed using Image-Pro Plus 6.0 software (Media Cybernetics, Inc.).

Reverse transcription-quantitative PCR (RT-qPCR). A high-purity RNA kit (Roche Diagnostics) was used for the isolation of total RNA from the RTECs and a spectrophotometer [Runqee (Shanghai) Instruments Technology Co., Ltd.)] was used to quantify the absorbance at 260 nm. Subsequently, 5 μl total RNA were reverse transcribed; cDNA was synthetized using the PrimeScript RT Reagent Kit (no. 6110A, Takara Bio, Inc.) as follows: 4 μl dNTP Mix, 2 μl Primer Mix and 7 μl RNA template were added to the tube and placed on the vibrator for full mixing, incubated at 70˚C for 10 min, and then rapidly washed on in ice for 2 min. Subsequently, 5X RT Buffer (4 μl), DTT (2 μl) and HiFiScript (1 μl) were added for full mixing, and incubated at 50˚C for 15 min, and then at 85˚C for 5 min. The mixture was then stored at -80˚C to prevent degradation. The cDNA was subjected to PCR using an ABI Prism 7000 sequence detector system (Applied Biosystems; Thermo Fisher Scientific, Inc.). PCR was conducted under the following conditions: 95˚C for 30 sec; 95˚C for 5 sec, 60˚C for 34 sec (40 cycles); and 95˚C, 5 sec, and 60˚C for 60 sec. The primer sequences used are listed in Table I (Mr. Yan-Fang Liu, research fellow from Tianjin Yishengyuan Biotechnology Co. Ltd. designed these sequences). The threshold cycle was obtained from triplicate samples and averaged. β-actin as an internal control for normalization. The calculations were based on the ΔΔCq method using the equation R (ratio)=$2^{-\Delta\Delta Cq}$ (19).

Statistical analysis. SPSS (IBM Corp.) statistical software (version 23.0) was used for statistical analysis. The measurement data of the normal distribution are expressed as mean ± standard deviation. The sample was repeated three times. Comparisons between groups were performed using one-way analysis of variance (ANOVA) followed by Tukey's post hoc test. Mitochondrial oxygen consumption was analyzed using two-way ANOVA followed by Bonferroni's post hoc test. Prism 8.3.0 software (GraphPad Software, Inc.) was used to plot the graphs. $P<0.05$ was considered to indicate a statistically significant difference.

Results

HO-1 regulates PINK1 in LPS-stimulated RTECs. Successful PINK1KO was established by the identification of the tail genotypes of F1 generation rats and the determination of

Table I. The primer sequences used in the present study.

Gene	Forward	Reverse
β-actin	5'-CGCGAGTACAACCTTCTTGC-3'	5'-ATACCCACCATCACACCCTG-3'
HO-1	5'-GACAGAGTTTCTTCGCCAGA-3'	5'-GCCACGGTCGCCAACAGGAA-3'
IL-1β	5'-TGTGGCAGCTACCTATGTCTT-3'	5'-AGTGCAGCTGTCTAATGGGAA-3'
Caspase1	5'-ACACCCACTCGTACACGTCTT-3'	5'-TTGTCATCTCCAGAGCTGTGA-3'
PINK1	5'-TACCGCTTCTTCCGCCAGTC-3'	5'-CGCCTGCTTCTCCTCGATCA-3'

PINK1 protein and mRNA expression (Figs. S1 and S2). PINK1 protein and mRNA were barely expressed in the PINK1KO RTECs (Fig. 2A, C and E). No significant differences were noted in the protein and mRNA expression levels of PINK1 between the LPS and hemin pre-treatment groups in the PINK1KO RTECs, which indicated that the PINK1 gene was knocked out. To confirm the association between HO-1 and PINK1 in LPS-stimulated RTECs, the expression levels of these proteins were determined in LPS-stimulated RTECs. The HO-1 and PINK1 protein and mRNA expression levels were upregulated when the RTECs were exposed to LPS. However, the HO-1 and PINK1 protein and mRNA expression levels were downregulated following pre-treatment of the cells with the HO-1 inhibitor, Znpp. The HO-1 and PINK1 protein and mRNA expression levels were upregulated following treatment of the cells with the HO-1 promoter and pre-treatment with hemin, which indicated that HO-1 promoted PINK1 expression (Fig. 2).

Effects of HO-1/PINK1 on RTEC viability. The effects of HO-1/PINK1 on RTEC viability were examined using CCK-8 assay (Fig. 3). In the WT RTECs, cell viability was decreased following exposure to LPS and even further decreased following pre-treatment with Znpp. By contrast, cell viability was increased following pre-treatment of the cells with hemin, which indicated that HO-1 promoted cell viability. However, the viability of the PINK1KO RTECs did not increase following pre-treatment with hemin, which indicated that HO-1 promoted cell viability via PINK1.

Effects of HO-1/PINK1 on inflammatory factors expressed in RTECs. RTEC injury is caused by the excessive release of inflammatory cytokines. To assess the anti-inflammatory effects of HO-1/PINK1, the expression levels of IL-6 and TNF-α were determined in the cell supernatant of RTECs (Fig. 4). In WT RTECs, the expression levels of IL-6 and TNF-α were increased following exposure of the cells to LPS. Furthermore, the expression levels of IL-6 and TNF-α were increased and decreased following pre-treatment of the cells with Znpp and hemin, respectively, indicating that HO-1 inhibited inflammatory cytokine release. However, the expression levels of IL-6 and TNF-α did not decrease following pre-treatment of PINK1KO RTECs with hemin, indicating that HO-1 inhibited inflammatory cytokine release via PINK1.

Effects of HO-1/PINK1 on the pyroptosis of RTECs. The induction of pyroptosis was investigated in RTECs using flow cytometry (Fig. 5). In the WT RTECs, the rate of pyroptosis was increased following stimulation of the cells with LPS. The rate of pyroptosis was increased following pre-treatment of the cells with Znpp and decreased following pre-treatment with hemin. However, the rate of pyroptosis did not decrease following pre-treatment of PINK1KO RTECs with hemin. This was consistent with the results of the flow cytometry experiments (Fig. 5A and B).

In addition, the protein and mRNA expression levels of caspase-1 and IL-1β were increased following stimulation of the cells with LPS. Furthermore, the protein and mRNA expression levels of caspase-1 and IL-1β were significantly increased following pre-treatment of the cells with Znpp compared with those noted in the LPS group. In contrast to these findings, the protein and mRNA expression levels of caspase-1 and IL-1β were decreased following pre-treatment of the cells with hemin. However, no significant differences were noted between the LPS and Hemin + LPS groups in the PINK1KO RTECs, which indicated that HO-1 did not inhibit the protein or mRNA expression levels of caspase-1 and IL-1β when PINK1 was knocked out. On the whole, these data indicated that HO-1 inhibited pyroptosis via PINK1.

Effects of HO-1/PINK1 on mitochondrial ROS in RTECs. To confirm the effects of HO-1/PINK1 on the mitochondrial function, the levels of mitochondrial ROS were detected in the RTECs (Fig. 6). In the WT RTECs, mitochondrial ROS levels increased following exposure to LPS compared with the control group. Furthermore, the ROS levels were increased and decreased following pre-treatment of the cells with Znpp and hemin respectively, compared with the LPS group, indicating that HO-1 reduced mitochondrial ROS levels. However, the ROS levels did not decrease following pre-treatment of PINK1KO cells with hemin, indicating that HO-1 inhibited mitochondrial ROS production via PINK1.

Effects of HO-1/PINK1 on mitochondrial ATP production in RTECs. To confirm the effects of HO-1/PINK1 on mitochondrial function, the mitochondrial ATP levels in RTECs were examined (Fig. 7). In the WT RTECs, the mitochondrial ATP levels were decreased following exposure of the cells to LPS. Furthermore, the mitochondrial ATP levels were decreased and increased following pre-treatment of the cells with Znpp and hemin, respectively, compared with the LPS group, which indicated that HO-1 promoted mitochondrial ATP production. However, the mitochondrial ATP levels were not increased following pre-treatment of PINK1KO RTECs with hemin, indicating that HO-1 promoted mitochondrial ATP production via PINK1.

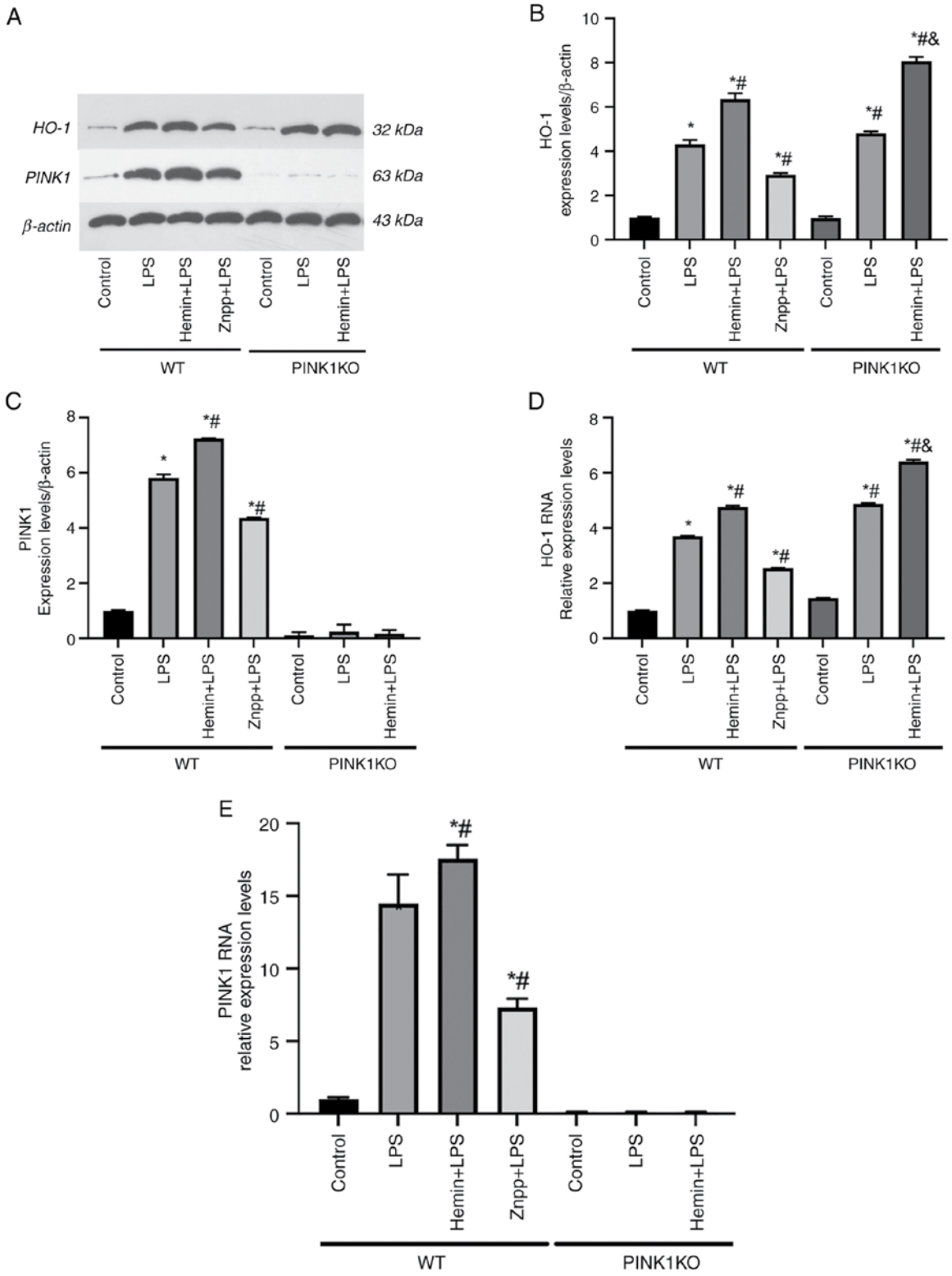

Figure 2. HO-1 regulates PINK1 in LPS-stimulated RTECs. (A) Representative western blots of HO-1 and PINK1. (B) Determination of the expression levels of HO-1 in RTECs. (C) Determination of the expression levels of PINK1 in RTECs. (D) Detection of HO-1 mRNA using reverse transcription-quantitative PCR. (E) mRNA expression levels of PINK1 in RTECs. The data are expressed as the mean ± SD, n=3. *P<0.05 vs. the WT control group, $^{\#}$P<0.05 vs. the WT LPS group, $^{\&}$P<0.05 vs. the PINK1KO LPS group. HO-1, heme oxygenase-1; PINK1, PTEN-induced putative kinase 1; LPS, lipopolysaccharide; RTECs, renal tubular epithelial cells; SD, standard deviation; WT, wild-type; KO, knockout; Znpp, zinc protoporphyrin IX.

Effects of HO-1/PINK1 on the mitochondrial respiratory function of RTECs. To confirm the effects of HO-1/PINK1 on mitochondrial function, the respiratory function of RTECs was investigated (Fig. 8). In the WT RTECs, the mitochondrial oxygen consumption was decreased following exposure of the cells to LPS. Furthermore, the mitochondrial oxygen consumption was decreased and increased following Znpp and hemin pre-treatment, respectively compared with the LPS group,

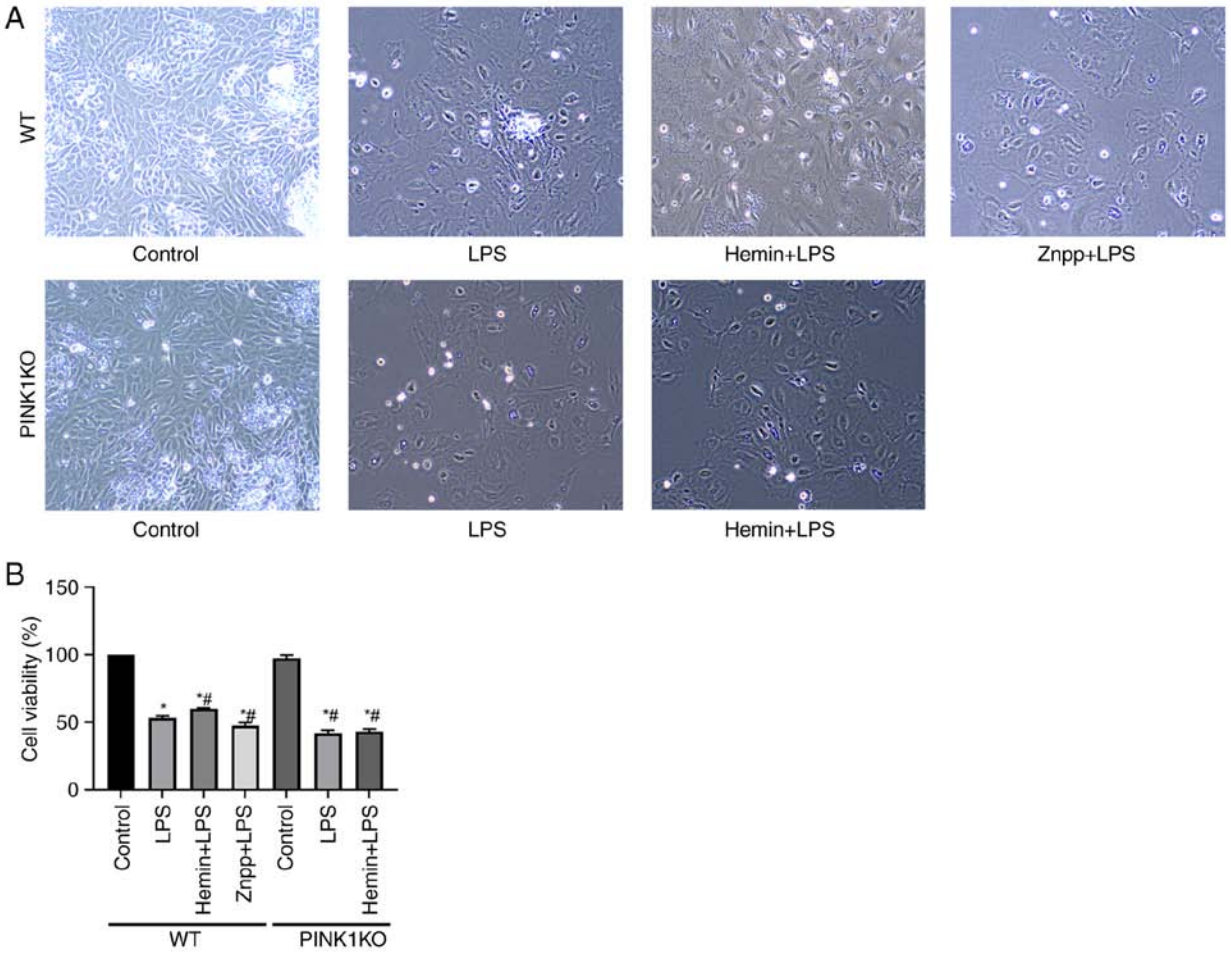

Figure 3. Effects of HO-1/PINK1 on RTEC viability. (A) Images of the activated state of cells observed under a microscope (magnification, x100). (B) Bar charts indicate the detection of cell viability. The data are expressed as the mean ± SD, n=3. *P<0.05 vs. the WT control group, #P<0.05 vs. the WT LPS group. HO-1, heme oxygenase-1; PINK1, PTEN-induced putative kinase 1; RTEC, renal tubular epithelial cell; SD, standard deviation; WT, wild-type; KO, knockout; LPS, lipopolysaccharide; Znpp, zinc protoporphyrin IX.

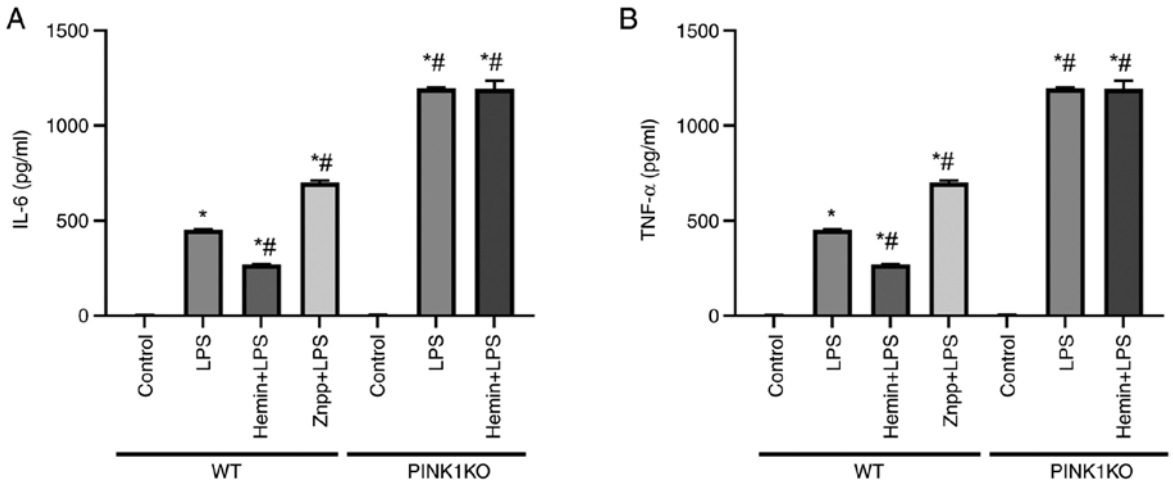

Figure 4. Effects of HO-1/PINK1 on the expression levels of inflammatory factors released in RTECs. (A) The levels of IL-6 in the cell supernatant. (B) The levels of TNF-α in the cell supernatant. The data are expressed as the mean ± SD, n=3. *P<0.05 vs. the WT control group, #P<0.05 vs. the WT LPS group. HO-1, heme oxygenase-1; PINK1, PTEN-induced putative kinase 1; RTECs, renal tubular epithelial cells; SD, standard deviation; WT, wild-type; KO, knockout; LPS, lipopolysaccharide; Znpp, zinc protoporphyrin IX.

which indicated that HO-1 promoted mitochondrial oxygen consumption. However, no significant difference was noted in the mitochondrial oxygen consumption between the LPS and Hemin + LPS groups in the PINK1KO RTECs. Collectively, these data indicated that HO-1 promoted mitochondrial oxygen consumption via PINK1.

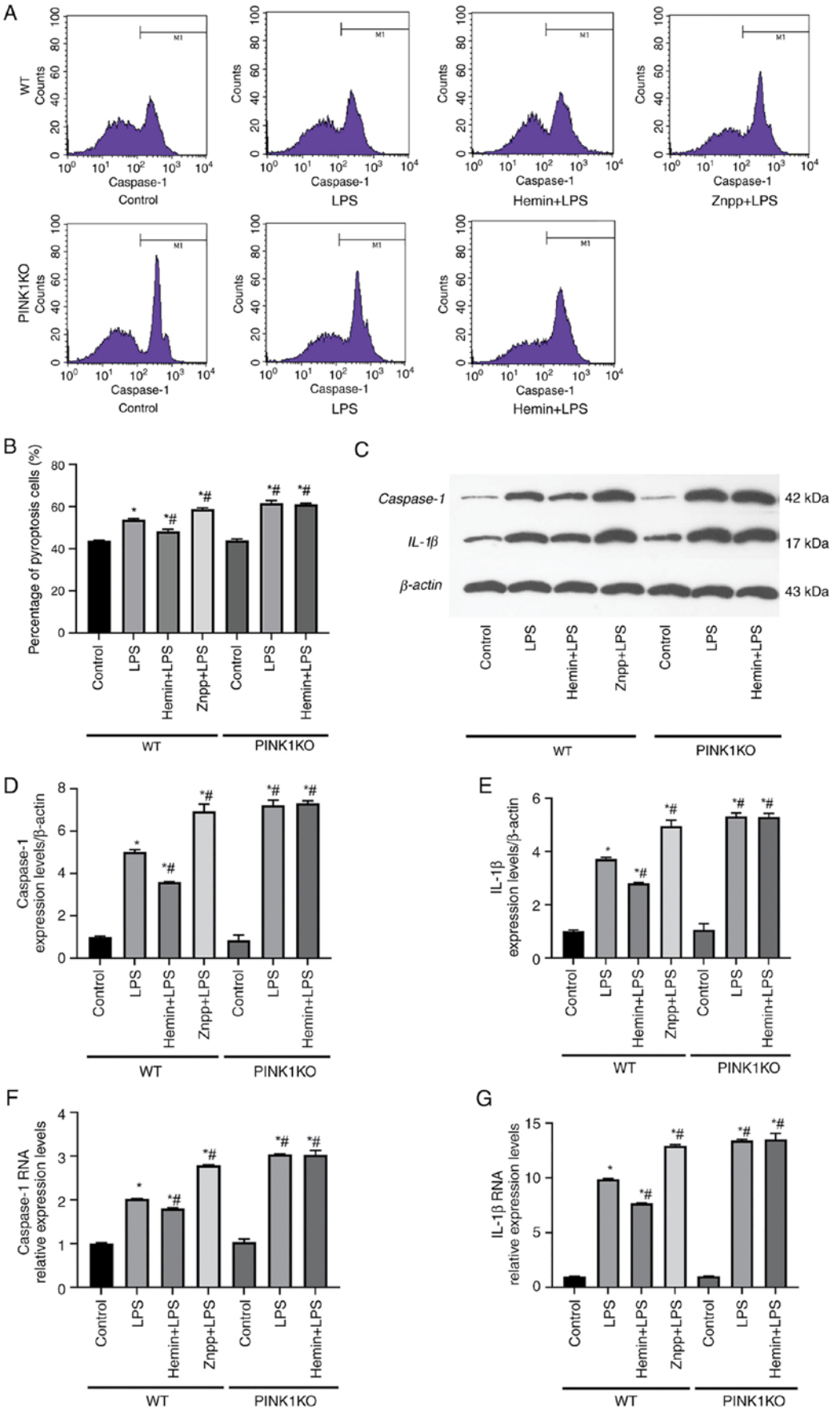

Figure 5. Effects of HO-1/PINK1 on the induction of the pyroptosis of RTECs. (A) Representative images of flow cytometry. (B) Percentage of pyroptosis-mediated RTEC damage. (C-E) Western blot analysis of the protein expression levels of caspase-1 and IL-1β in RTECs. (F and G) Reverse transcription-quantitative PCR results indicating the relative mRNA expression levels of caspase-1 and IL-1β. The data are expressed as the mean ± SD, n=3. *P<0.05 vs. the WT control group, $^{\#}$P<0.05 vs. the WT LPS group. HO-1, heme oxygenase-1; PINK1, PTEN-induced putative kinase 1; RTECs, renal tubular epithelial cells; SD, standard deviation; WT, wild-type; KO, knockout; LPS, lipopolysaccharide; Znpp, zinc protoporphyrin IX.

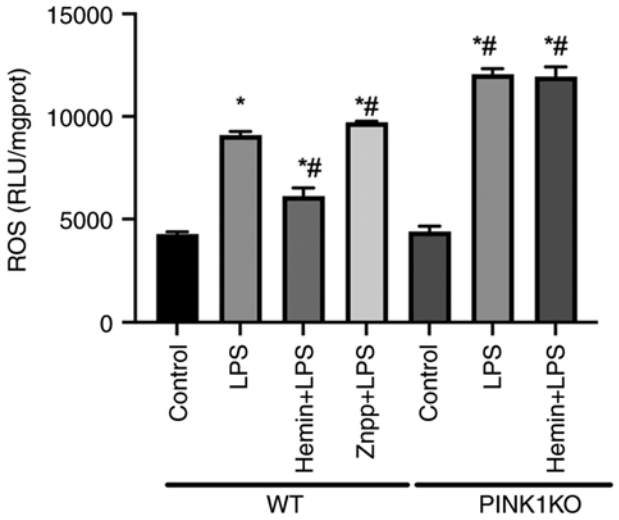

Figure 6. Effects of HO-1/PINK1 on mitochondrial ROS levels in RTECs. The mitochondrial ROS levels were assessed in RTECs. The data are expressed as the mean ± SD, n=3. *P<0.05 vs. the WT control group, #P<0.05 vs. the WT LPS group. HO-1, heme oxygenase-1; PINK1, PTEN-induced putative kinase 1; ROS, reactive oxygen species; RTECs, renal tubular epithelial cells; SD, standard deviation; WT, wild-type; KO, knockout; LPS, lipopolysaccharide; Znpp, zinc protoporphyrin IX.

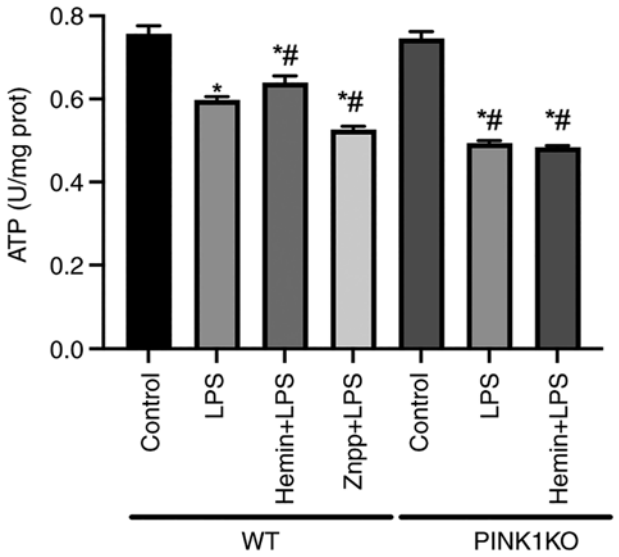

Figure 7. Effects of HO-1/PINK1 on mitochondrial ATP levels in RTECs. Determination of the mitochondrial ATP levels in RTECs. The data are expressed as the mean ± SD, n=3. *P<0.05 vs. the WT Control group, #P<0.05 vs. the WT LPS group. HO-1, heme oxygenase-1; PINK1, PTEN-induced putative kinase 1; ATP, adenosine triphosphate; RTECs, renal tubular epithelial cells; SD, standard deviation; WT, wild-type; KO, knockout; LPS, lipopolysaccharide; Znpp, zinc protoporphyrin IX.

Discussion

The primary culture of RTECs can be achieved by sieve centrifugation. The separation of the glomerulus and renal tubules can be performed by grinding of the renal tissue and filtering using a mesh, and the exclusion of glomerulus cells can be performed using 80- and 100-mesh screens, which can obtain more RTECs and make them purer (20). Under a microscope (optical), the RTECs exhibit a multilateral cobblestone shape, and the cells are closely connected (21). In the present study, primary cultured RTECs were also multilateral cobble-like under a microscope (optical), and the cells were closely connected; thus, it was confirmed that the cultured cells were RTECs.

AKI caused by endotoxemia is relatively common in clinical practice (2,22,23). Among the common pathogenic bacteria that cause endotoxemia, Gram-negative bacteria are the most common and cause endotoxemia by secreting LPS (24). Therefore, LPS was selected in the present study to induce endotoxemia in RTECs. An LPS concentration of 1 μg/ml can lead to RTEC injury (25). Therefore, the present study used an LPS concentration of 1 μg/ml to prepare the LPS-induced RTEC injury model. The changes in sex hormone levels may have an effect on endotoxemia. Male rats are affected at different levels by endotoxins compared with female rats. It has been shown that in the presence of toxins and hematic disease caused by shock, male rats are more likely to develop immunosuppression, which leads to their inability to tolerate AKI. In contrast to male rats, female rats can tolerate AKI due to the increased levels of estrogen (26). Therefore, although the present study involved mainly *in vitro* experiments, male rats were selected in order to reduce the effect of estrogen on RTECs. The results indicated that the viability of the RTECs was decreased and the expression levels of the inflammatory cytokines, IL-6 and TNF-α, were increased following exposure of the cells to LPS. These findings indicated the successful establishment of the model used in the present study.

RTEC injury plays a crucial role in the pathogenesis of AKI (5,27). RTEC injury is mainly manifested by cell necrosis and apoptosis; the pyroptosis of RTECs has been recently discovered (6,28). Therefore, RTEC pyroptosis was observed in the present study. Pyroptosis is a form of programmed necrotizing death that is primarily mediated by caspase-1 and leads to the activation of IL-1β (8,9,29,30). Therefore, the expression levels of caspase-1 and IL-1β were detected in the present study. The data indicated that the expression levels of caspase-1 and IL-1β were increased along with the rate of pyroptosis of the RTECs following their exposure to LPS, which indicated that LPS induced the pyroptosis of RTECs.

Mitochondria are considered the core organelles of cellular energy metabolism and consequently, mitochondrial dysfunction is a main cause of pyroptosis (31). Mitochondria produce ATP through a complex of electron respiratory chains, which provide energy for cells (12). Mitochondrial damage leads to mitochondrial dysfunction; consequently, ATP synthesis decreases, ROS production increases and the mitochondrial oxygen consumption rate decreases, leading to cell necrosis, apoptosis and pyroptosis (10,32,33). *In vivo* research has indicated that the mitochondrial fission of endotoxemia induces the pyroptosis of RTECs and causes AKI (11). In the present study, ATP production and ROS levels were increased following the stimulation of isolated RTECs with LPS, whereas the mitochondrial oxygen consumption rate was decreased, indicating mitochondrial dysfunction.

HO-1 exerts endogenous protective effects and can protect multiple organs against damage caused by endotoxemia (16,34,35). The protection from toxin release by endogenous HO-1 expression in AKI was also confirmed

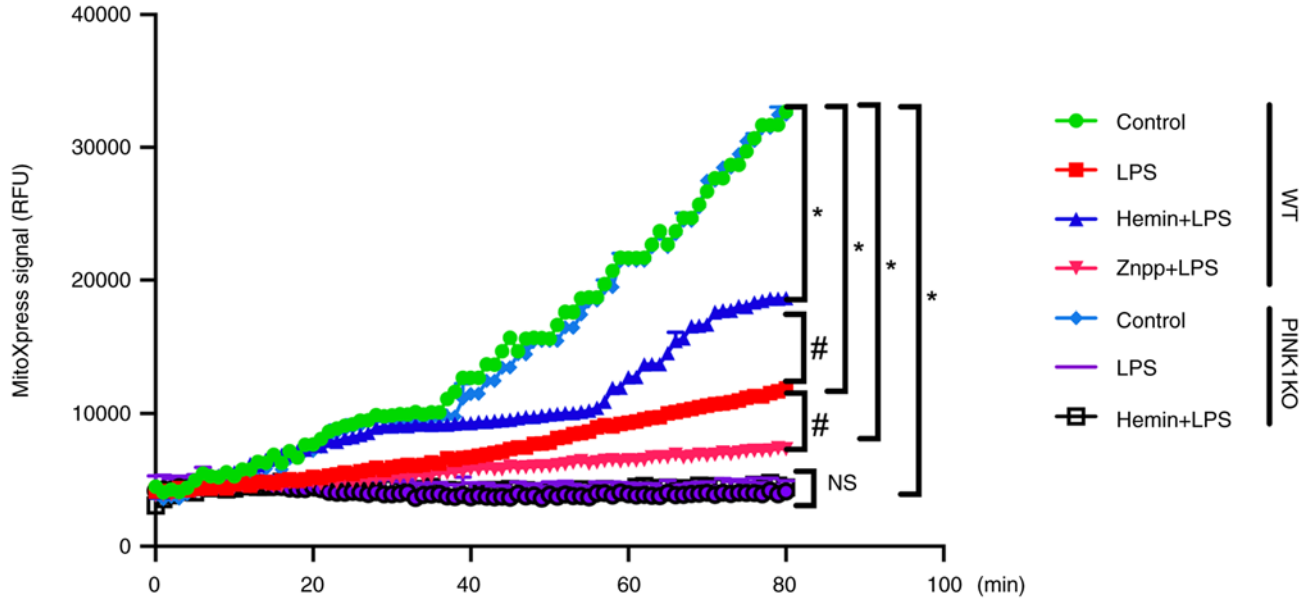

Figure 8. Effects of HO-1/PINK1 on the mitochondrial respiratory function in RTECs. The data are expressed as the mean ± SD, n=3. *P<0.05 vs. the WT control group, #P<0.05 vs. the WT LPS group. NS, not significant; HO-1, heme oxygenase-1; PINK1, PTEN-induced putative kinase 1; RTECs, renal tubular epithelial cells; SD, standard deviation; WT, wild-type; KO, knockout; LPS, lipopolysaccharide; Znpp, zinc protoporphyrin IX.

in a previous *in vivo* study by the authors (11). The HO-1 mRNA and protein levels in the kidneys have been shown to be upregulated in rats following stimulation by lipopolysaccharide (34). The HO-1 mRNA and protein levels RTECs were upregulated following stimulation with LPS in the present study. This type of protection is not only reflected in its effect on mitochondrial dynamics. By contrast, HO-1 exerts antiapoptotic, antioxidant and anti-inflammatory functions, and assists in maintaining cellular homeostasis and function by playing a critical role in the process (36-39). In the present study, it was found that the upregulation of HO-1 expression inhibited the production of inflammatory factors, while it increased ATP synthesis, decreased ROS levels, increased mitochondrial oxygen consumption, inhibited pyroptosis, and increased the viability of RTECs. The inhibition of HO-1 expression exerted the opposite effects. These results suggested that HO-1 inhibited the inflammatory response, improved mitochondrial function, inhibited pyroptosis, and attenuated the injury to LPS-stimulated RTECs. Previous *in vivo* studies have shown that HO-1 regulates mitochondrial fusion/fission through PINK1, inhibits pyroptosis and improves endotoxemia in AKI; PINK1 can regulate mitochondrial autophagy, remove damaged mitochondria and improve mitochondrial function (40-42). The present study investigated the induction of pyroptosis, mitochondrial dysfunction, and the upregulation of PINK1 expression in LPS-stimulated RTECs *in vitro*. When HO-1 was upregulated, the expression levels of PINK1 were also upregulated, whereas when the expression of HO-1 was inhibited, the expression of PINK1 was downregulated; this indicated that HO-1 expression regulated PINK1 and that HO-1 was involved in the regulation of mitochondrial function. When PINK1 expression was knocked out, HO-1 expression was upregulated and its effect in regulating mitochondrial function was weakened. This further

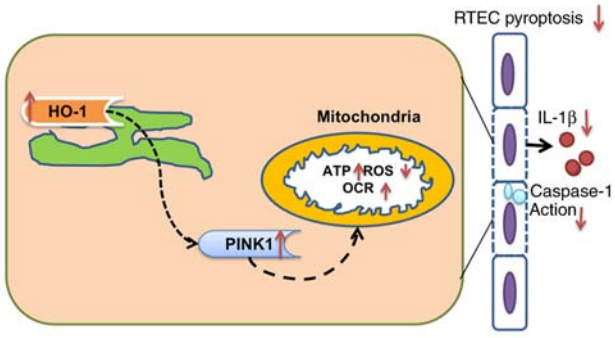

Figure 9. Schematic diagram indicating the pathophysiological pathway leading to pyroptosis.

demonstrated that HO-1 regulated mitochondrial function, inhibited pyroptosis, and enhanced the viability of RTECs via PINK1.

The present study is based on previous findings, which mainly discussed the influence of the HO-1/PINK1 pathway on mitochondrial fusion/division *in vivo* (11). The innovation of the present study was the *in vitro* culture of RTECs, and the verification of the influence of the HO-1/PINK1 pathway on mitochondrial function. The present study has several limitations, however. Firstly, it was observed that AKI was induced only 6 h following stimulation of the cells with LPS; therefore, additional time points are required to further explore the induction of this disease. Secondly, the effects of various concentrations of LPS on RTECs need to be determined. Thirdly, mitochondrial function was only noted in RTECs; however, mitochondrial morphology needs to be determined. Fourthly, mitochondrial dysfunction inhibiting pyroptosis needs to be investigated using a mitochondrial dysfunction inhibitor. Lastly, in order to illustrate the HO-1-mediated regulation of PINK1 more efficiently, PINK1 overexpression

should be verified. In the PINK1KO RTECs, the setting of the LPS + ZnPP group will provide more information. In addition, only HO-1 inhibitors were used to alter the expression of HO-1, which would be more effective to verify the results if the changes were made at the gene level by using siRNA or overexpression plasmids. Previous research has demonstrated that electroacupuncture can inhibit the inflammatory response and oxidative stress in sepsis and improve acute kidney injury (43). Whether electroacupuncture can attenuate RTEC injury through HO-1/PINK1 is worthy of further investigation. Additional studies are required to investigate the mechanisms underlying the HO-1/PINK1 interaction in endotoxin-stimulated RTECs.

In conclusion, the present study demonstrated that HO-1 inhibited the inflammatory response, improved mitochondrial function, and inhibited the pyroptosis of LPS-stimulated RTECs, which may be related to PINK1 (Fig. 9).

Acknowledgements

The authors would like to thank Mr. Yan-Fang Liu (research fellow from Tianjin Yishengyuan Biotechnology Co. Ltd.) for providing technical assistance.

Funding

The present study was financially supported by the Inner Mongolia Natural Science Foundation (grant no. 2021MS08061).

Availability of data and materials

The datasets used and/or analyzed during the current study are available from the corresponding author on reasonable request.

Authors' contributions

HBL, YSM and XZZ contributed to the preparation of the manuscript and the overall study design. QZ, XDL and JNS contributed to data analysis. LNH, JNW, YG and DDF performed the experiments. JBY and YS contributed to the overall study design and performed a critical review of the manuscript. All authors have read and approved the final version of the manuscript and confirm the authenticity of all the raw data.

Ethics approval and consent to participate

The present study was approved by the Animal Ethical and Welfare Committee of the Institute of Radiation Medicine, Chinese Academy of Medical Sciences (no. IRM-DWLL-201907) and was performed in accordance with the ARRIVE guidelines developed by the National Center for the Replacement, Refinement, and Reduction of Animals in Research.

Patient consent for publication

Not applicable.

Competing interests

The authors declare that they have no competing interests.

References

1. Lai TS, Wang CY, Pan SC, Huang TM, Lin MC, Lai CF, Wu CH, Wu VC and Chien KL; National Taiwan University Hospital Study Group on Acute Renal Failure (NSARF): Risk of developing severe sepsis after acute kidney injury: A population-based cohort study. Crit Care 17: R231, 2013.
2. Weng L, Zeng XY, Yin P, Wang LJ, Wang CY, Jiang W, Zhou MG and Du B; China Critical Care Clinical Trials Group (CCCCTG): Sepsis-related mortality in China: A descriptive analysis. Intensive Care Med 44: 1071-1080, 2018.
3. Poston JT and Koyner JL: Sepsis associated acute kidney injury. BMJ 364: k4891, 2019.
4. Messaris E, Memos N, Chatzigianni E, Kataki A, Nikolopoulou M, Manouras A, Albanopoulos K, Konstadoulakis MM and Bramis J: Apoptotic death of renal tubular cells in experimental sepsis. Surg Infect (Larchmt) 9: 377-388, 2008.
5. Priante G, Gianesello L, Ceol M, Del Prete D and Anglani F: Cell death in the kidney. Int J Mol Sci 20: 3598, 2019.
6. Ye Z, Zhang L, Li R, Dong W, Liu S, Li Z, Liang H, Wang L, Shi W, Malik AB, *et al*: Caspase-11 mediates pyroptosis of tubular epithelial cells and septic acute kidney injury. Kidney Blood Press Res 44: 465-478, 2019.
7. Bergsbaken T, Fink SL and Cookson BT: Pyroptosis: Host cell death and inflammation. Nat Rev Microbiol 7: 99-109, 2009.
8. Man SM, Karki R and Kanneganti TD: Molecular mechanisms and functions of pyroptosis, inflammatory caspases and inflammasomes in infectious diseases. Immunol Rev 277: 61-75, 2017.
9. Jorgensen I, Rayamajhi M and Miao EA: Programmed cell death as a defence against infection. Nat Rev Immunol 17: 151-164, 2017.
10. Sedlackova L and Korolchuk VI: Mitochondrial quality control as a key determinant of cell survival. Biochim Biophys Acta Mol Cell Res 1866: 575-587, 2019.
11. Li HB, Zhang XZ, Sun Y, Zhou Q, Song JN, Hu ZF, Li Y, Wu JN, Guo Y, Zhang Y, *et al*: HO-1/PINK1 regulated mitochondrial fusion/fission to inhibit pyroptosis and attenuate septic acute kidney injury. Biomed Res Int 2020: 2148706, 2020.
12. Pfanner N, Warscheid B and Wiedemann N: Mitochondrial protein organization: From biogenesis to networks and function. Nat Rev Mol Cell Biol 20: 267-284, 2019.
13. Supinski GS, Schroder EA and Callahan LA: Mitochondria and critical illness. Chest 157: 310-322, 2020.
14. Bolisetty S, Zarjou A and Agarwal A: Heme oxygenase 1 as a therapeutic target in acute kidney injury. Am J Kidney Dis 69: 531-545, 2017.
15. Suliman HB, Keenan JE and Piantadosi CA: Mitochondrial quality-control dysregulation in conditional HO-1$^{-/-}$ mice. JCI Insight 2: e89676, 2017.
16. Chen X, Wang Y, Xie X, Chen H, Zhu Q, Ge Z, Wei H, Deng J, Xia Z and Lian Q: Heme oxygenase-1 reduces sepsis-induced endoplasmic reticulum stress and acute lung injury. Mediators Inflamm 2018: 9413876, 2018.
17. Tang C, Han H, Yan M, Zhu S, Liu J, Liu Z, He L, Tan J, Liu Y, Liu H, *et al*: PINK1-PRKN/PARK2 pathway of mitophagy is activated to protect against renal ischemia-reperfusion injury. Autophagy 14: 880-897, 2018.
18. Ding W, Yousefi K and Shehadeh LA: Isolation, characterization, and high throughput extracellular flux analysis of mouse primary renal tubular epithelial cells. J Vis Exp: 57718, 2018.
19. Livak KJ and Schmittgen TD: Analysis of relative gene expression data using real-time quantitative PCR and the 2(-Delta Delta C(T)) method. Methods 25: 402-408, 2001.
20. Mattila PM, Nietosvaara YA, Ustinov JK, Renkonen RL and Häyry PJ: Antigen expression in different parenchymal cell types of rat kidney and heart. Kidney Int 36: 228-233, 1989.
21. Van Kooten C, Lam S and Daha MR: Isolation, culture, characterization and use of human renal tubular epithelial cells. J Nephrol 14: 204-210, 2001.
22. Shankar-Hari M, Phillips GS, Levy ML, Seymour CW, Liu VX, Deutschman CS, Angus DC and Rubenfeld GD: Developing a new definition and assessing new clinical criteria for septic shock: For the third international consensus definitions for sepsis and septic shock (sepsis-3). JAMA 315: 775-787, 2016.

23. Cecconi M, Evans L, Levy M and Rhodes A: Sepsis and septic shock. Lancet 392: 75-87, 2018.
24. Plotnikov EY, Brezgunova AA, Pevzner IB, Zorova LD, Manskikh VN, Popkov VA, Silachev DN and Zorov DB: Mechanisms of LPS-induced acute kidney injury in neonatal and adult rats. Antioxidants (Basel) 7: 105, 2018.
25. Quoilin C, Mouithys-Mickalad A, Duranteau J, Gallez B and Hoebeke M: Endotoxin-induced basal respiration alterations of renal HK-2 cells: A sign of pathologic metabolism down-regulation. Biochem Biophys Res Commun 423: 350-354, 2012.
26. Tang YQ and Li L: Development strategy and application of animal model of sepsis. Chin J Exp Surg 12: 1433-1434, 2006 (In Chinese).
27. Peerapornratana S, Manrique-Caballero CL, Gómez H and Kellum JA: Acute kidney injury from sepsis: Current concepts, epidemiology, pathophysiology, prevention and treatment. Kidney Int 96: 1083-1099, 2019.
28. Chen F, Lu J, Yang X, Xiao B, Chen H, Pei W, Jin Y, Wang M, Li Y, Zhang J, *et al*: Acetylbritannilactone attenuates contrast-induced acute kidney injury through its anti-pyroptosis effects. Biosci Rep 40: BSR20193253, 2020.
29. Shi J, Zhao Y, Wang Y, Gao W, Ding J, Li P, Hu L and Shao F: Inflammatory caspases are innate immune receptors for intracellular LPS. Nature 514: 187-192, 2014.
30. Broz P: Immunology: Caspase target drives pyroptosis. Nature 526: 642-643, 2015.
31. Friedman JR and Nunnari J: Mitochondrial form and function. Nature 505: 335-343, 2014.
32. Yu W, Sheng M, Xu R, Yu J, Cui K, Tong J, Shi L, Ren H and Du H: Berberine protects human renal proximal tubular cells from hypoxia/reoxygenation injury via inhibiting endoplasmic reticulum and mitochondrial stress pathways. J Transl Med 11: 24, 2013.
33. Murphy MP and Hartley RC: Mitochondria as a therapeutic target for common pathologies. Nat Rev Drug Discov 17: 865-886, 2018.
34. Yu JB, Zhou F, Yao SL, Tang ZH, Wang M and Chen HR: Effect of heme oxygenase-1 on the kidney during septic shock in rats. Transl Res 153: 283-287, 2009.
35. Yin H, Li X, Yuan B, Zhang B, Hu S, Gu H, Jin X and Zhu J: Heme oxygenase-1 ameliorates LPS-induced acute lung injury correlated with downregulation of interleukin-33. Int Immunopharmacol 11: 2112-2117, 2011.
36. Abraham NG, Lin JH, Schwartzman ML, Levere RD and Shibahara S: The physiological significance of heme oxygenase. Int J Biochem 20: 543-558, 1988.
37. Gozzelino R, Jeney V and Soares MP: Mechanisms of cell protection by heme oxygenase-1. Annu Rev Pharmacol Toxicol 50: 323-354, 2010.
38. Kozakowska M, Dulak J and Józkowicz A: Heme oxygenase-1-more than the cytoprotection. Postepy Biochem 61: 147-158, 2015 (In Polish).
39. Cai ZY, Sheng ZX and Yao H: Pachymic acid ameliorates sepsis-induced acute kidney injury by suppressing inflammation and activating the Nrf2/HO-1 pathway in rats. Eur Rev Med Pharmacol Sci 21: 1924-1931, 2017.
40. Bayne AN and Trempe J: Mechanisms of PINK1, ubiquitin and parkin interactions in mitochondrial quality control and beyond. Cell Mol Life Sci 76; 4589-4611, 2019.
41. Lin Q, Li S, Jiang N, Shao X, Zhang M, Jin H, Zhang Z, Shen J, Zhou Y, Zhou W, *et al*: PINK1-parkin pathway of mitophagy protects against contrast-induced acute kidney injury via decreasing mitochondrial ROS and NLRP3 inflammasome activation. Redox Biol 26: 101254, 2019.
42. Leites EP and Morais VA: Mitochondrial quality control pathways: PINK1 acts as a gatekeeper. Biochem Biophys Res Commun 500: 45-50, 2018.
43. Yu JB, Shi J, Zhang Y, Gong LR, Dong SA, Cao XS, Wu LL and Wu LN: Electroacupuncture ameliorates acute renal injury in lipopolysaccharide-stimulated rabbits via induction of HO-1 through the PI3K/Akt/Nrf2 pathways. PLoS One 10: e0141622, 2015.